Digital Object Identifier: 10.1109/ULTSYM.2008.0176

Study on Acoustical Physical Constants of ZnO Single Crystal Using the Ultrasonic Microspectroscopy Technology

Tomoya Tanaka, Yuji Ohashi, Mototaka Arakawa, Jun-ichi Kushibiki, and Noboru Sakagami
Department of Electrical and Communication Engineering
Tohoku University
Sendai, Japan
kushi@ecei.tohoku.ac.jp

***Abstract*—This paper describes an investigation of determining acoustical physical constants of ZnO. We obtained three specimens of (001)-, (100)-, and (101)-ZnO crystal substrates prepared from three very small single crystals, grown by the hydrothermal synthesis method. We measured bulk-wave velocities in the frequency range from 50 MHz to 300 MHz and LSAW velocities at 225 MHz using the ultrasonic microspectroscopy (UMS) technology. We observed that the specimens included partially conductive region inside the crystals. We determined the constants more accurately except for e_{15} and e_{31}.**

Keywords-ZnO single crystal; ultrasonic microspectroscopy technology; acoustical physical constants; leaky surface acoustic wave velocity; bulk wave velocity

I. INTRODUCTION

ZnO is one of famous piezoelectric materials and has been widely used as ultrasonic transducers and surface-acoustic-wave (SAW) devices [1-6]. Accurate acoustical physical constants (elastic constants, piezoelectric constants, dielectric constants, and density) of actually employed crystals are necessary for developing and designing ultrasonic devices.

We have been studying the development and application of ultrasonic microspectroscopy (UMS) technology with a line-focus-beam (LFB) / plane-wave (PW) ultrasonic-material-characterization (UMC) system [4, 7, 8]. So far, we have developed methods of evaluating the elastic homogeneity of single crystals and wafers such as $LiNbO_3$, $LiTaO_3$, and α-quartz and of determining their acoustical physical constants [9-11]. Recently we have begun to extend and apply our system for ZnO and AlN crystals [12, 13]. Both the crystals belongs to class 6mm of the hexagonal system. In our previous report [12], we detected variations in acoustic properties for ZnO single crystals due to differences in conductivity. Such effect causes a problem for determining accurate acoustical physical constants.

In this paper, we preliminary determined the acoustical physical constants of ZnO single crystals using three specimens of (001)-, (100)-, and (101)-ZnO crystal substrates through measurements of bulk-wave velocities and leaky-surface-acoustic-wave (LSAW) velocities.

II. SPECIMENS

We prepared three specimens of (001)- (*Z*-cut), (100)- (*Y*-cut), and (101)- (28.39°*Y*-cut) ZnO crystal substrates, naturally grown crystalline surfaces, from three small single crystals grown by the hydrothermal synthesis method [14]. The dimensions were 6×9×2.4696 mm^3 for a *Z*-cut specimen, 7×11×3.1641 mm^3 for a *Y*-cut specimen, and 10×11×2.6 mm^3 for a 28.39°*Y*-cut specimen. Both of the top and bottom surfaces of each specimen were optically polished with parallelism of less than 0.01°.

III. EXPERIMENTS

The LSAW velocity V_{LSAW} was obtained through the V(z) curve measurement by the LFB-UMC system [4, 7]. The measurement method and system were presented in detail in the literature [4]. A (110)Ge was used as a standard specimen for the system calibration [15] because its LSAW propagation characteristics were close to those for ZnO single crystals. V_{LSAW} was measured at 225 MHz and its measurement reproducibility was about $\pm 2\sigma = \pm 0.2$ m/s (σ: standard deviation).

To confirm homogeneities in acoustic properties on the specimen surface, two-dimensional distributions of LSAW velocities were measured for both of the top and bottom surfaces of each specimen. Average V_{LSAW} around the central area of the specimens (2×2 mm^2) was 2669.0 m/s with a maximum variation of 0.4 m/s on the top surface of the *Z*-cut specimen and 2668.3 m/s with a maximum variation of 2.5 m/s on the bottom surface. On both surfaces for the *Z*-axis propagation on the *Y*-cut specimen, we obtained almost the same average velocity value of 2644.6 m/s with a maximum variation of 0.4 m/s. Comparing these results and calculated results using the published constants [16], the *Z*-cut and *Y*-cut specimens were estimated to have high resistivity, but the bottom surface of the Z-cut specimen might have a little bit lower resistivity. Fig. 1 shows the measurement result of a two-dimensional distribution of 90°*X*-propagating LSAW velocity on the top surface of the 28.39°*Y*-cut specimen. Average V_{LSAW} on the top surface was 2785.3 m/s with a maximum variation of 0.8 m/s within an area of 1×1 mm^2 indicated by the black dotted line in Fig. 1 where the measured

velocities might be for a highly resistive specimen surface. In the V_{LSAW} distribution, we observed a low velocity region with an average velocity value of 2707.1 m/s with a maximum variation of 0.3 m/s for a scanning area of 1×1 mm^2 indicated by the white dotted line in Fig. 1. We also observed low V_{LSAW} distribution for the whole area on the bottom surface of the 28.39°*Y*-cut specimen reflecting low resistivity, and obtained averaged V_{LSAW} of 2708.2 m/s with a maximum variation of 2.7 m/s. We used the information of the LSAW velocities for the resistive and conductive surfaces. So we did not use this (101) specimen for bulk-wave velocity measurements because of homogeneity problem.

Bulk-wave velocities, longitudinal and shear velocities, were measured for the *Z*-cut and *Y*-cut substrate specimens in a frequency range from 50 to 300 MHz by the PW-UMC system [8]. We could not observe any velocity dispersions in results for *Y*-axis propagating longitudinal wave V_{Yl}, *Y*-axis propagating shear wave with *X*-axis polarized particle displacement V_{YsX}, and *Z*-axis propagating shear wave V_{Zs} which did not couple with the piezoelectricity. Figs. 2 and 3 show the results for the *Z*-axis propagating longitudinal wave V_{Zl} and *Y*-axis propagating shear wave with *Z*-axis polarized particle displacement V_{YsZ} which couple with the piezoelectricity. We observed significant velocity dispersions of 2 m/s for V_{Zl} and 1 m/s for V_{YsZ} in the measurement frequency range. We also obtained large velocity differences of 2.7 m/s in Fig. 2 and 32.3 m/s in Fig. 3 at 225 MHz between the measured and calculated values. It is considered that these velocity dispersions result from the relaxation due to the conductivity of the ZnO specimens. Therefore we can conclude that the *Z*-cut and *Y*-cut specimens could include a material region with partially low resistivity on the way of bulk-wave propagation.

Table I summarizes the measured velocities of longitudinal and shear waves, and LSAWs at 225 MHz, together with the calculated values for both bulk-wave and LSAW modes using the published constants [16]. We can see significant differences between the measured and calculated values. All the measured LSAW velocities were in good agreement with the calculated values. The bulk wave velocities of V_{Zl},V_{Yl}, and V_{Zs} agree well with the calculated values, while those of V_{YsX} and V_{YsZ} are by 10.8 m/s and 32.3 m/s, respectively, lower than the calculated values.

IV. Discussion

Next, we try to determine all of the acoustical physical constants using the measured results. First of all, we could estimate V_{Zl} as 6375 m/s from Fig. 2, and V_{YsZ} as 2797.5 m/s from Fig. 3 at much higher frequencies. We employ the V_{Zl} value of 6101.7 m/s for the very conductive Z-cut specimen measured previously [12]. We also use the bulk-wave velocity values of V_{Yl}, V_{YsX}, and V_{Zs} not coupling with the piezoelectricity, and two LSAW velocities at two positions with high and low resistivities for the 28.39°*Y*-cut specimen. In the determination process of the constants, we used the values of density and dielectric constants in the literature [16]. The constants c_{11}^E, c_{12}^E, c_{33}^E, c_{44}^E, e_{15}, and e_{33} were determined from only bulk wave velocities, c_{44}^E was obtained from the relation that $\rho V_{Zs}^2 = c_{44}^E$, and c_{33}^E was obtained from the V_{Zl} of 6101.7 m/s for the conductive Z-cut specimen. Then e_{15} and e_{33} determined from the relations that $\rho V_{YsZ}^2 = c_{44}^E + e_{15}^2 / \varepsilon_{11}^S$ and $\rho V_{Zl}^2 = c_{33}^E + e_{33}^2 / \varepsilon_{33}^S$. The remaining constant c_{13}^E was determined using the LSAW velocity of 2707.1 m/s at the

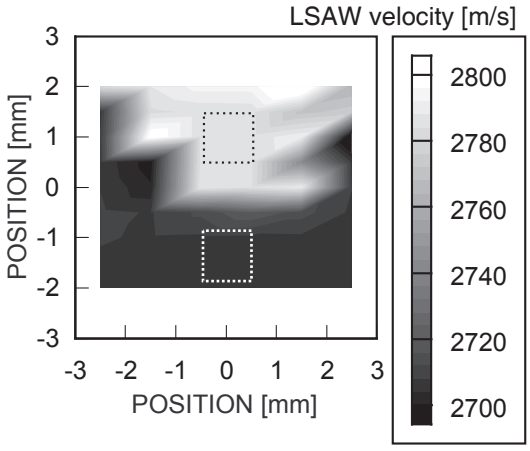

Figure 1. LSAW velocity distribution for 28.39°*Y*-cut 90°*X*-prop. ZnO single crystal at 225 MHz.

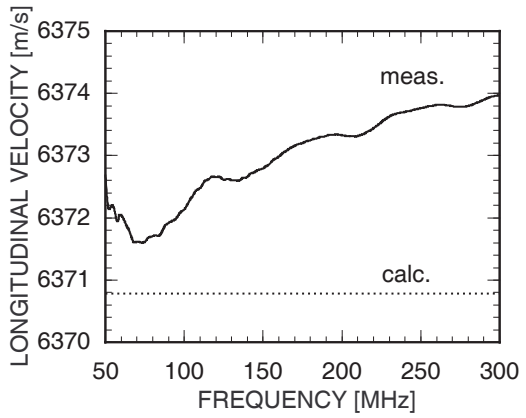

Figure 2. *Z*-prop. longitudinal wave velocities.

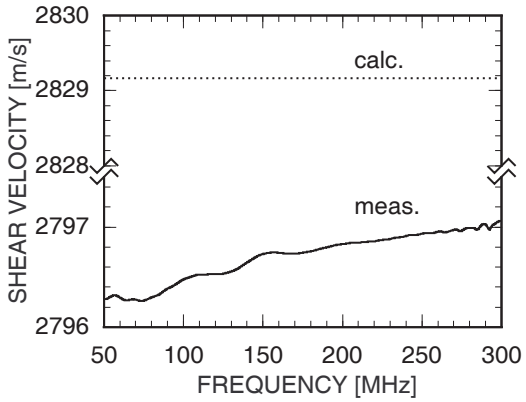

Figure 3. *Y*-prop. *Z*-pol. shear wave velocities.

TABLE I. COMPARISON OF MEASURED AND CALCULATED VELOCITIES FOR ZNO SINGLE CRYSTALS.

Mode	Plane	Prop.	Pol.	Velocity [m/s]		
				$V_{meas.}$	$V_{calc.}$	$V_{meas.} - V_{calc.}$
Longitudinal wave	*Z*	*Z*	-	6373.5	6370.8	2.7
	Y	*Y*	-	6078.0	6082.7	-4.7
Shear wave	*Z*	*Z*	-	2734.6	2732.6	2.0
	Y	*Y*	*X*	2793.5	2804.3	-10.8
	Y	*Y*	*Z*	2796.9	2829.2	-32.3
LSAW	*Z*	-	-	2669.0	2672.9	-3.9
	Y	*Z*	-	2644.6	2644.7	-0.1
	28.39°*Y*	90°*X*	-	2785.3	2785.1	0.2

TABLE II. COMPARISON OF DETERMINED AND PUBLISHED CONSTANTS OF ZNO SINGLE CRYSTALS.

Constant		Determined	Published [16]	Difference [%]
Elastic Constant [$\times 10^{11}$ N/m^2]	c_{11}^E	2.093	2.096	-0.14
	c_{12}^E	1.209	1.205	0.33
	c_{13}^E	1.057	1.046	1.05
	c_{33}^E	2.109	2.106	0.14
	c_{44}^E	0.4236	0.423	0.14
Piezoelectric Constant [C/m^2]	e_{15}	-0.386	-0.480	-19.6
	e_{31}	-0.713	-0.573	24.4
	e_{33}	1.321	1.321	0.00

conductive position of the 28.39°*Y*-cut specimen and the predetermined constants c_{11}^E, c_{12}^E, c_{33}^E, c_{44}^E, and ρ, and finally the constant e_{31}, using the LSAW velocity of 2785.3 m/s at the resistive position. Table II shows the acoustical physical constants determined and the published constants [16]. We believe that we could determine the more accurate constants for actually employed ZnO crystals, although there are still some considerable errors for e_{15} and e_{31}.

V. CONCLUSION

We measured bulk wave velocities and LSAW velocities for three ZnO single crystal specimens using the LFB/PW-UMC system. The experimental results suggested that these specimens had partially conductive regions. We tentatively determined acoustical physical constants of ZnO single crystal from measured velocities. Further investigation will be conducted for determining the constants for ZnO single crystals with higher resistivity.

ACKNOWLEDGMENT

This work was supported in part by a Research Grant-in-Aid for the Global Center of Excellence (COE) Program funded by the Ministry of Education, Culture, Sports, Science and Technology, Japan.

REFERENCES

[1] N. Chubachi, M. Minakata, and Y. Kikuchi, "Physical structure of DC diode sputtered ZnO films and its influence on the effective electromechanical coupling factors," Jpn. J. Appl. Phys., Vol. 2, Suppl. 2-1, pp. 737-740, 1974.

[2] N. Chubachi, "ZnO film concave transducer for focusing radiation of microwave ultrasound," Electron. Lett., Vol. 12, pp. 595-596, 1976.

[3] N. Chubachi, "ZnO films for surface acoustopic devices on nonpiezoelectric substrates," Proc. IEEE, Vol. 64, pp. 772-773, 1976.

[4] J. Kushibiki and N. Chubachi, "Material characterization by line-focus-beam acoustic microscope," IEEE Trans. Sonics Ultrason., Vol. SU-32, No. 2, pp. 189-212, Mar. 1985.

[5] F. S. Hickernell, "Zinc oxide films for acoustoelectric device applications," IEEE Trans. Sonics Ultrason., Vol. SU-32, No. 5, pp. 621-629, Sep. 1985.

[6] M. Kadota, C. Kondo, T. Ikeda, and T. Kasanami, "Frequency trimming of ZnO/Glass SAW filters," Jpn. J. Appl. Phys., Vol. 30, pp. 179-181, 1991.

[7] J. Kushibiki, Y. Ono, Y. Ohashi, and M. Arakawa, "Development of the line-focus-beam ultrasonic material characterization system," IEEE Trans. Ultrason., Ferroelect., Freq. Contr., Vol. 49, No. 1, pp. 99-113, Jan. 2002.

[8] J. Kushibiki and M. Arakawa, "Diffraction effects on bulk-wave ultrasonic velocity and attenuation measurements," J. Acoust. Soc. Am., Vol. 108, No. 2, pp. 564-573, Aug. 2000.

[9] J. Kushibiki, Y. Ohashi, and J. Hirohashi, "Ultrasonic microspectroscopy of congruent $LiNbO_3$ crystals," J. Appl. Phys., Vol. 98, 123507, Dec. 2005.

[10] J. Kushibiki and Y. Ohashi, “Determination of the true congruent composition for $LiTaO_3$ single crystals using the LFB ultrasonic material characterization system," IEEE Trans. Ultrason., Ferroelectr., Freq. Contr., Vol. 53, No. 2, pp. 385-392, Feb. 2006.

[11] J. Kushibiki, I. Takagana, and S. Nishiyama, “Accurate measurements of the acoustical physical constants of synthetic α-quartz for SAW devices,” IEEE Trans. Ultrason., Ferroelectr., Freq. Contr., Vol. 49, No. 1, pp. 125-135, Jan. 2002.

[12] T. Tanaka, Y. Ohashi, M. Arakawa, and J. Kushibiki, "Evaluation of ZnO single crystals by means of the ultrasonic microspectroscopy technology," IEICE Tech. Rep., Vol. 107, No. 233, US2007-51, pp. 49-54, Sep. 2007.

[13] Y. Ohashi, M. Arakawa, J. Kushibiki, B. M. Epelbaum, and A. Winnacker, ”Ultrasonic microspectroscopy characterization of AlN single crystals,” Appl. Phys. Express, Vol. 1, 077004, July 2008.

[14] T. Sekiguchi, S. Miyashita, K. Obata, T. Shishido, and N. Sakagami, "Hydrothermal growth of ZnO single crystals and their optical characterization," J. Cryst. Growth, Vol. 214/215, pp. 72-76, 2000.

[15] J. Kushibiki and M. Arakawa, "A method of calibrating the line-focus-beam acoustic microscopy system", IEEE Trans. Ultrason., Ferroelectr., Freq. Contr., Vol. 45, No. 2, pp. 421-430, Mar. 1998.

[16] R. T. Smith and V. E. Stubblefield, “Temperature dependence of the electroacoustical constants of Li-doped ZnO single crystals,” J. Acoust. Soc. Am., Vol. 45, p. 105, 1969.